Impact of RF Stress on Dispersion and Power Characteristics of AlGaN/GaN HEMTs

Shawn S.H. Hsu, Pouya Valizadeh, Dimitris Pavlidis
Department of Electrical Engineering and Computer Science,
The University of Michigan, Ann Arbor, MI 48109-2122, USA
Tel: (734) 647-1778, Fax: (734) 763-6132, email: pavlidis@umich.edu, http://www.eecs.umich.edu/dp-group
J. S. Moon, M. Micovic, D. Wong and T. Hussain
HRL Laboratories, 3011 Malibu Canyon Road, Malibu, CA 90265, USA

Abstract

The impact of RF stress on dispersion and power characteristics of AlGaN/GaN HEMTs are reported. Reduced drain current (~ 67 mA/mm in the saturation region) and similar output power and Power-Added Efficiency were found after RF stress. Transconductance dispersion is small before and after RF stress while output resistance dispersion reduces after RF stress. Tests performed under UV light suggest that the observed results may be attributed to trapping in the AlGaN/GaN HEMT layers.

I. Introduction

AlGaN/GaN HEMTs have been reported with superior output power characteristics [1]. However, current instability and dispersion effects have been reported to be present in such wide bandgap devices as demonstrated by various experiments [2-4]. The observed characteristics of AlGaN/GaN HEMTs are not well understood at this point and their power performance often deviates from DC predicted characteristics. It is consequently very important to understand and if possible to control and suppress such effects to improve the power performance of GaN-based devices. In this work, the impact of RF stress on the dispersion of output resistance (R_{DS}) and transconductance (g_m), as well as the power characteristics of AlGaN/GaN HEMTs was studied. Load-pull and dispersion measurements were used for this purpose. In addition, UV light was employed to examine the current instability and dispersion effects of RF-stressed devices.

Section II describes the DC and microwave characteristics of AlGaN/GaN HEMTs. Section III compares the device *I-V* characteristics and microwave power performance before and after RF stress. Section IV presents the impact of RF stress on R_{DS} and g_m dispersion effects. Section V shows the impact of UV light on the *I-V* curve and power characteristics of RF-stressed devices.

II. DC and Microwave Characteristics

The layers of the AlGaN/GaN HEMTs studied here were grown on 4H-SiC substrates using RF-assisted MBE. The devices had a gate length of 0.25 μm and a total gate finger width of 150 μm. A peak transconductance of ~ 170 mS/mm was observed. The device showed maximum oscillation frequency (f_{max}) of ~ 95 GHz and cut-off frequency (f_T) of ~ 50 GHz at V_{GS} ~ -3.0 to -3.5 V. Fig. 1 shows the dependence of f_{max} and f_T on the gate and drain bias voltages. As can be seen, the devices show good microwave characteristics under a wide range of bias conditions, which provide flexibility for circuit applications.

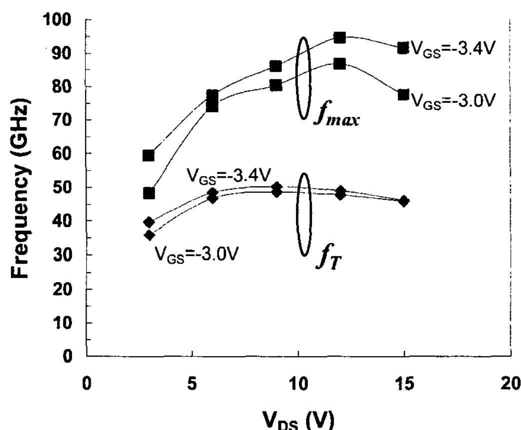

Fig. 1: Dependence of f_{max} and f_T on bias conditions for 0.25×150 μm^2 AlGaN/GaN HEMTs.

III. Impact of RF Stress on DC and Microwave Power Characteristics

Fig.2 shows the DC *I-V* characteristics for devices before and after RF stress. RF stress was performed using a 5 GHz microwave source delivering a power of 20 dBm to the gate of the device. The current was found to reduce and the pinch-off voltage became less negative after RF stress. This could possibly be associated with the presence of traps in AlGaN/GaN HEMTs. Under large RF signal, carriers may be excited and fill up such traps. In case of acceptor-type traps, these become negative charged after being filled and act as a second gate [5]. They are consequently presenting an additional negative voltage on the gate, and therefore a less negative gate voltage is necessary to pinch off the device, as shown by the experimental results.

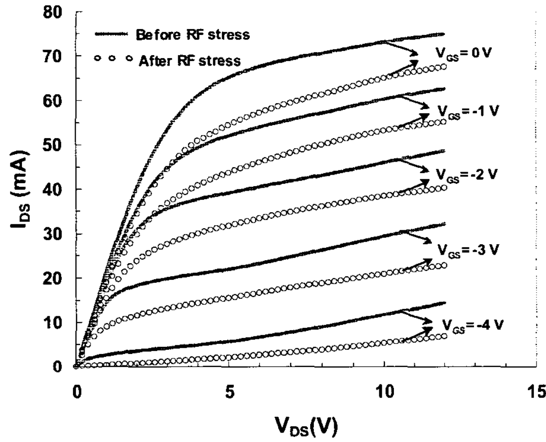

Fig. 2: *I-V* characteristics of 0.25×150 μm^2 AlGaN/GaN HEMTs before and after RF stress.

Load-pull measurements were performed under input and output matching conditions at 5 GHz. Fig. 3 shows the power characteristics before and after RF stress. The device was biased at V_{GS}= -3V, and V_{DS}= 12 V. At low input power levels, one can see that I_{DS} reduces by ~ 10 mA after RF stress. In addition, as the input power level increases, the drain current is found to gradually reduce before RF stress, while after RF stress, the I_{DS} variation is relatively small. Despite the presented I_{DS} variation, the device shows only slight reduction of gain, P_{out}, and PAE. As mentioned above, the variation of I_{DS} may be attributed to filling up of traps due to carrier excitation. This introduces negative charges and an additional gate negative voltage which lead in a smaller effective carrier concentration. Since these traps have very long time constants, their presence manifests in changes of DC characteristics but their impact on microwave performance is relatively small.

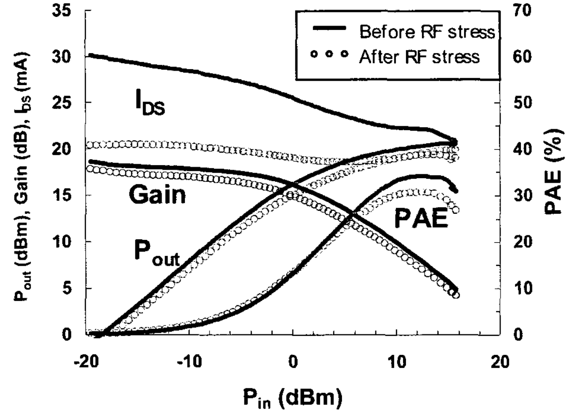

Fig. 3: Power characteristics and I_{DS} of 0.25×150 μm^2 AlGaN/GaN HEMTs before and after RF stress.

IV. Dispersion of Output Resistance and Transconductance

The dispersion of output resistance was measured by applying a DC voltage to the gate, while an AC signal with a DC voltage offset was used for the drain bias. The dispersion effects can be measured directly from the AC voltage across a sensing resistor at the drain terminal. A similar setup with AC signal applied to the gate side was used for transconductance dispersion measurements. The measurement was performed in the frequency range of 50 Hz to 100 kHz.

Fig. 4 shows the transconductance dispersion after RF stress. Since the extrinsic g_m is closely related to the source access resistance, the g_m measurement can be used to evaluate the dispersion characteristics of the gate-source lateral region. Very little dispersion of transconductance was observed for both cases before and after RF stress, which suggests that the traps of the device are not located in the gate-source region. The latter also agrees with the fact that carriers accelerate along the channel and attain high energy within the gate-drain area.

Therefore, carriers are more likely to participate in the trapping-detrapping process in the vicinity of the drain terminal. The pronounced dispersion effects of R_{DS} shown below support this assumption.

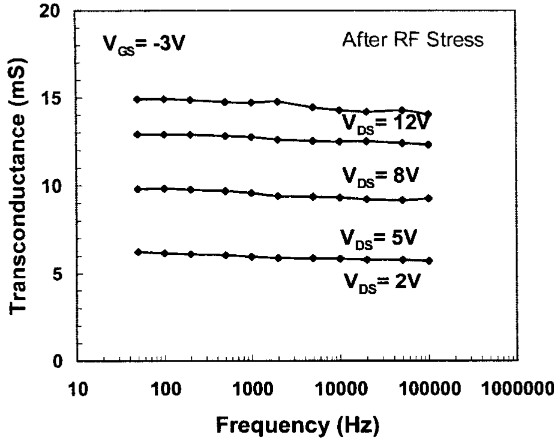

Fig. 4: Frequency-dependent transconductance of 0.25×150 μm^2 AlGaN/GaN HEMTs from 50 Hz to 100 kHz after RF stress.

Fig. 5 shows the output resistance dispersion before and after RF stress at V_{GS}= -3 V and under different V_{DS}. Dispersion of R_{DS} was observed before and after RF stress and the devices showed smaller output resistance dispersion after RF stress. Considering that R_{DS} is related to the number of carriers in the channel when V_{DS} changes, the reduced R_{DS} dispersion implies smaller carrier variation after RF stress. Since traps are likely to be filled up after RF excitation, there are less traps available for the carrier trapping-detrapping process. As a result, less R_{DS} dispersion was observed after RF stress.

V. Impact of UV Light on RF-stressed Devices

To investigate the trapping effects on wide bandgap GaN-based devices, high power UV light was applied to the RF-stressed devices. UV light contains photons with energy higher than the bandgap of GaN, and therefore it can be used to excite deep level traps in the GaN-based devices. Fig. 6 compares the *I-V* characteristics before RF stress and after RF stress followed by exposure to continuous UV light. Under strong

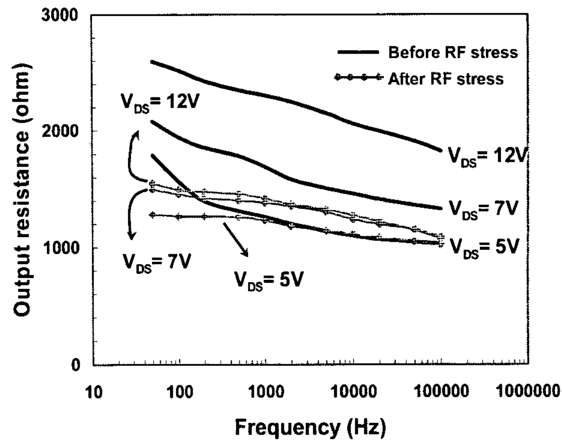

Fig. 5: Frequency-dependent output resistance of 0.25×150 μm^2 AlGaN/GaN HEMTs from 50 Hz to 100 kHz before and after RF stress.

UV light, the trapped carriers are fully excited, and therefore the additional negative charges introduced by traps are eliminated, with the result of increased drain current. As can be seen, the drain current is completely recovered from the reduction due to RF stress and becomes even higher than the value before RF stress. The result suggests that traps may be partially filled before RF excitation. Moreover, the reduction of I_{DS} after RF stress appears to be mainly related to traps rather than a permanent damage of the device.

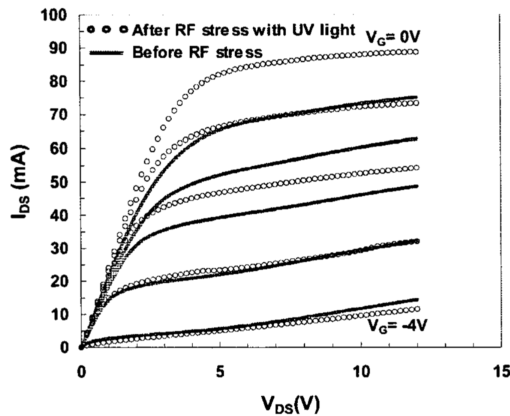

Fig.6: DC *I-V* characteristics of 0.25×150 μm^2 AlGaN/GaN HEMTs before RF stress and after RF stress followed by UV light exposure.

Fig. 7 compares the power characteristics of devices before RF stress and after RF stress followed by exposure to continuous UV light. As can be seen, the output power and gain are similar, while I_{DS} and PAE are different. The drain current I_{DS} is higher and reduces at a slower rate after exposure to UV light. This is due to traps, which are no longer filled eliminating therefore the virtual gate effects. A further reduction of I_{DS} is observed at input power level exceeding ~ 10 dBm. This occurs with and without UV light exposure and is related to thermal effects. On the other hand, the reduced PAE can be ascribed to the increased drain current level with UV light. Since P_{out} and gain are similar, a higher drain current translates in a higher DC power consumption and therefore a lower PAE.

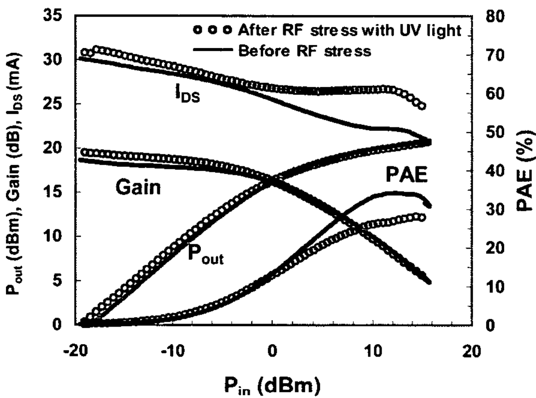

Fig.7: Power characteristics of 0.25×150 μm² AlGaN/GaN HEMTs before RF stress and after RF stress followed by UV light exposure.

VI. Conclusion

Overall, the impact of RF stress on AlGaN/GaN HEMTs was investigated by means of microwave power and low-frequency dispersion measurements. The devices present a significant DC current change after RF power stress. However, only small variation was observed for microwave power characteristics. Filled up traps with long time constants due to RF excitation may be responsible for this finding. The dispersion measurements suggest that traps are mainly located in the gate-drain area and less traps are available for the trapping-detrapping process after RF stress. In addition, devices tested under UV light show drain current recovery indicating that the trapping effects are responsible for the observed characteristics. The results help to identify the origin of current instability and dispersion effects of AlGaN/GaN HEMTs and lead to further improvement of the device performance.

Acknowledgement: work supported by ONR (contract nos.N00014-00-1-0879, N00014-02-1-0128) and HRL Laboratories. The authors are grateful to Drs. J. Zolper and H. Dietrich for technical discussions and support of this work.

[References]

[1] L. Shen, S. Heikman, B. Moran, R. Coffie, N.-Q Zhang, D. Buttari, I. P. Smorchkova, S. Keller, S. P. DenBaars, U.K. Mishra, "AlGaN/AlN/GaN high-power microwave HEMT," *IEEE Electron Device Letters*, vol. 22, no. 10, pp. 457-459, Oct. 2001.

[2] S. Hsu, P.N. Tan, D. Pavlidis, E. Alekseev, N.X. Nguyen, C. Nguyen, and D.E. Grider, "Frequency dependent output resistance and transconductance in ALGaN/GaN MODFETs," Proceeding of 1999 International Semiconductor Device Research Symposium (ISDRS), Charlottesville, Virginia, pp. 315-317, Dec., 1999.

[3] E. Kohn, I. Daumiller, P. Schmid, N. X. Nguyen, "Large signal frequency dispersion of AlGaN/GaN heterostructure field effect transistors," *Electronics Lett.*, vol. 35, no.12, June 1999.

[4] I. Daumiller, D. Theron, C. Gaquiere, A. Vescan, R. Dietrich, A. Wieszt, H. Leier, R. Vetury, U. K. Mishra, I. P. Smorchkova, N. X. Nguyen, C. Nguyen, and E. Kohn, "Current instabilities in GaN-based devices," *IEEE Electron Device Lett.*, vol. 22, no.2, Feb. 2001.

[5] R. Vetury, N. Q. Zhang, S. Keller, and U. K. Mishra, "The Impact of Surface States on the DC and RF Characteristics of AlGaN/GaN HFETs," *IEEE Trans. Electron Devices, vol. 48, No. 3, pp. 560–566, Mar. 2001*